



'On/off'-switchable catalysis by a smart enzyme-like imprinted polymer

Songjun Li^{a,b,*}, Yi Ge^{b,*}, Ashutosh Tiwari^b, Shenqi Wang^b, Anthony P.F. Turner^b, Sergey A. Piletsky^b

^aKey Laboratory of Pesticide & Chemical Biology of Ministry of Education, College of Chemistry, Central China Normal University, Wuhan 430079, China

^bCranfield Health, Vincent Building, Cranfield University, Cranfield, Bedfordshire MK43 0AL, UK

ARTICLE INFO

Article history:

Received 22 October 2010

Revised 11 November 2010

Accepted 12 November 2010

Available online 14 January 2011

Keywords:

Catalysis

Smart materials

Modulation

Imprinted catalyst

ABSTRACT

'On/off'-switchable catalysis by a smart enzyme-like imprinted polymer is reported. This unique imprinted polymer was composed of poly(*N*-isopropylacrylamide)-containing *p*-nitrophenyl phosphate-imprinted networks that exhibited temperature-dependent hydrophilicity/hydrophobicity. At a relatively low temperature (such as 20 °C), this polymer was capable of vigorous catalysis for the hydrolysis of *p*-nitrophenyl acetate due to its hydrophilic networks, which enabled access to the imprinted framework. On the contrary, at higher temperatures (such as 40 °C), this polymer demonstrated poor catalysis resulting from its dramatically increased hydrophobicity, which inhibited access to the imprinted sites. Unlike previously reported imprinted polymers which lack adjustable networks, this novel imprinted polymer employed thermosensitive poly(*N*-isopropylacrylamide) networks, thus enabling the switchable catalysis.

Crown Copyright © 2010 Published by Elsevier Inc. All rights reserved.

1. Introduction

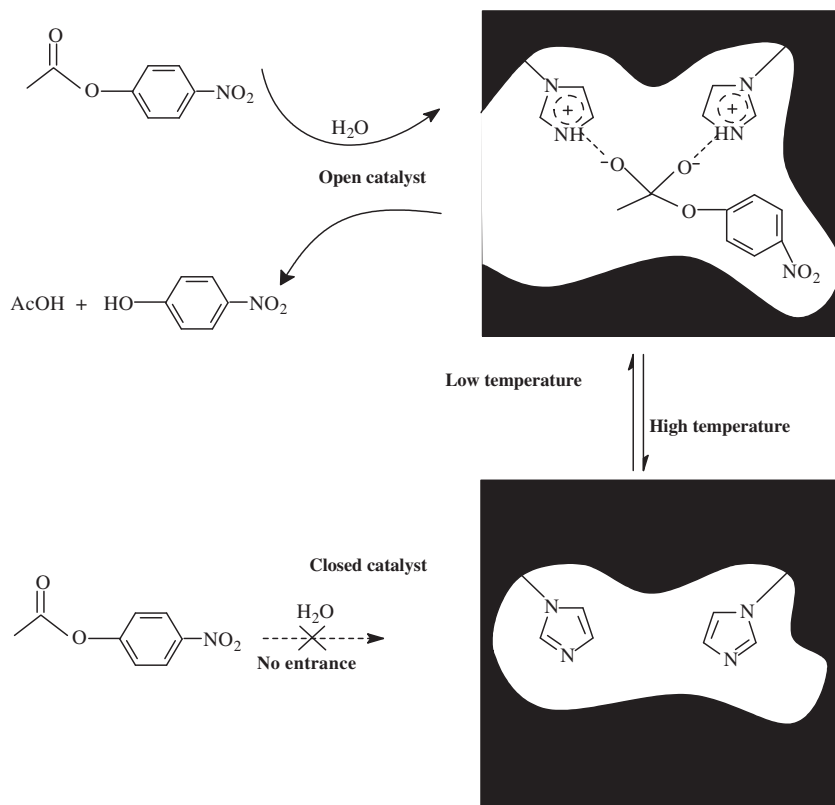
The appeal of developing biomimetic catalytic materials capable of recognizing and catalyzing desired molecules is gaining traction, because of their importance in a broad range of applications [1–3]. Prominent among the ongoing endeavor is the application of molecular imprinting technique, which provides a straightforward route to develop molecular recognition and catalytic materials comparable to natural antibodies but with improved properties [4,5]. Known as a 'from-key-to-lock' technology, molecular imprinting is capable of tailor-made binding sites for desired templates within highly cross-linked polymers. In order to fabricate molecularly imprinted polymers, the template and functional monomers are first allowed to form a self-assembled architecture where the functional monomers are regularly positioned around the template. Polymerization is then performed to fix this self-organized architecture in place, followed by removal of the imprinted template from the polymeric networks, which thereby leaves behind binding sites stereochemically complementary to the template. In this way, the match between the template and binding sites constitutes an induced molecular memory, thus enabling the prepared polymer to recognize the imprint species (*i.e.*, the template). For their application in enzyme-like catalysis, a template similar to the transition-state of the ongoing reaction, *i.e.*, transition-state analogue (TSA), is generally used [6]. The rea-

son for this is related to the phenomenon that activation energy is usually needed to overcome the potential barrier between the reactant and product (*i.e.*, the conversion from the reactant state to the transition-state) [7]. As such, the host–guest interaction within the molecular imprinting system is generally comparable to that within natural biosystems, such as enzyme–substrate, receptor–ligand and antibody–antigen. However, compared with these biosystems, molecularly imprinted polymers are highly cross-linked polymers, which thus offer significant advantages including resistance to elevated temperature and pressure, and inertia to acid, base, metal ion, organic solvent, etc. Hence, molecularly imprinted polymers are especially suitable to be used as molecular recognition and catalytic materials under harsh conditions.

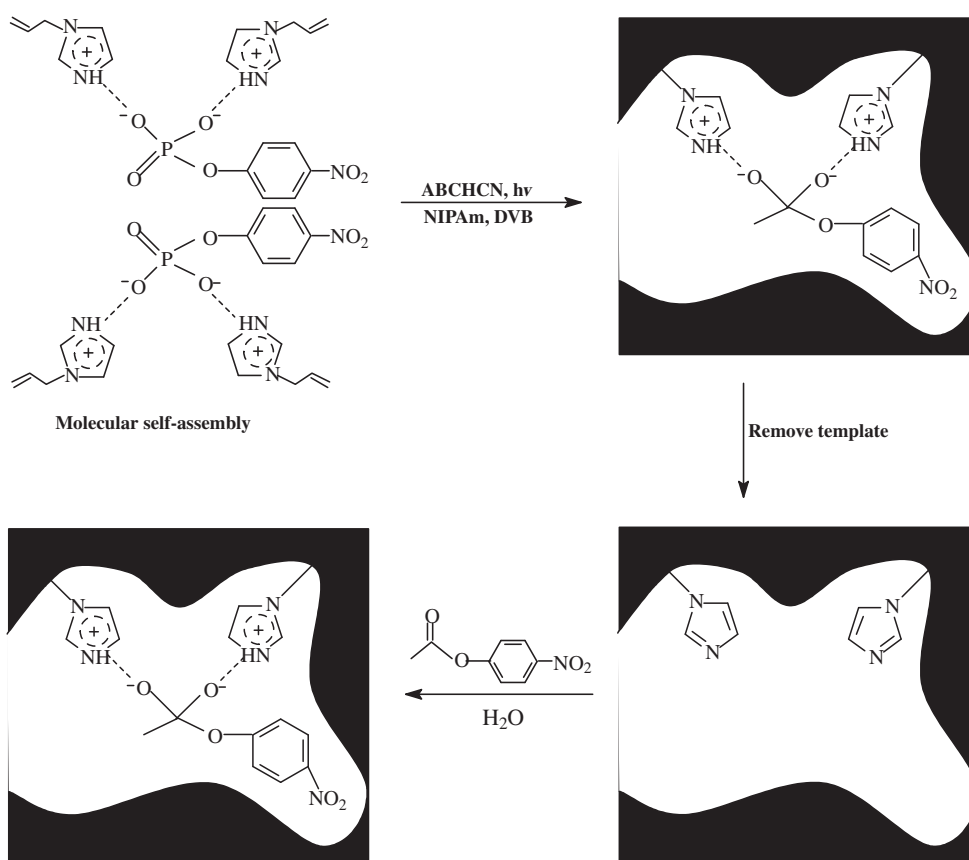
One emerging frontier in chemical research is to handle chemical reactions into an adjustable model. Scientists in this field have been working to cater for this challenge over the past few years [8–10]. Prominent among them are Bergbreiter and his colleagues [11,12], who have greatly contributed to this field by developing poly(*N*-isopropylacrylamide) (PNIPAm)-bound catalysts. By using the unique thermosensitive phase transition of PNIPAm, catalysts or substrates bound upon PNIPAm can be readily recovered by using heating (water) or solvent precipitation, which thus led this system to a smart catalytic one capable of quantitative isolation of catalysts. Now, it is clear that these results can be directly attributed to the unique structure of PNIPAm, which comprises hydrophilic amide chains and hydrophobic isopropyl. At a temperature below its lower critical solution temperature (LCST; ~32 °C), the polymer is soluble in water due to the hydrogen-bonding interactions between the amide chains and water [13]. At a

* Corresponding authors. Address: Key Laboratory of Pesticide & Chemical Biology of Ministry of Education, College of Chemistry, Central China Normal University, Wuhan 430079, China (S. Li). Fax: +44 (0) 1234758380.

E-mail addresses: Lsjchem@yahoo.com.cn (S. Li), y.ge@cranfield.ac.uk (Y. Ge).



Scheme 1. Proposed mechanism for the modulated catalysis by MIP-S.



Scheme 2. Scheme for the preparation of MIP-S.

temperature above the LCST, the polymer is subject to a thermal phase transition induced by the suppression of hydrogen-bonding interactions, resulting in dramatically increased hydrophobicity [14]. Encouraged by these elegant works, we [15] and related researchers [16,17] have successfully developed molecularly imprinted polymers capable of thermosensitive molecular recognition. At relative low temperatures, the polymers can specifically recognize their templates due to the hydrophilic networks, which enable access for analytes in waters to the imprinted sites. Above the transition temperature, the dramatically increased hydrophobicity causes shrinking of the imprinted networks, destroying the molecular recognition ability. In this way, molecular recognition by such smart imprinted polymers demonstrated the temperature-dependent adjustable model.

Inspired by this mechanism, we herein report the first example of switched catalysis by a smart and enzyme-like imprinted polymer (namely ‘MIP-S’). As illustrated in Scheme 1, below the LCST, the hydrophilic imprinted networks allow access to the reactants, thereby enabling catalysis. On the contrary, above the LCST, the dramatically decreased hydrophilicity causes shrinking of the imprinted networks, which inhibits the reactivity of this polymer. Thus, the temperature-regulated catalysis by MIP-S can be recognized as an ‘on/off-switchable process. In order to test such switchable catalytic properties, the hydrolysis of *p*-nitrophenyl acetate (NPA) was selected as the model reaction, because this reaction is compatible with water and has a well-proven TSA (i.e., *p*-nitrophenyl phosphate; NPP) [18,19]. For the study of catalytic specificity, *p*-nitrophenyl butyrate (NPB), the structural analogue of NPA, was selected as the control. The objective of this study is to demonstrate that modulated catalysis can be realized by utilizing a smart and catalytic imprinted polymer.

2. Experimental section

2.1. Preparation of imprinted polymers

Unless otherwise noted, chemicals were obtained from Aldrich (Sigma–Aldrich Company Ltd., Dorset, UK) and Fisher (Fisher Scientific UK Ltd., Loughborough, UK) and used as received, except 1-vinylimidazole (VI) and divinylbenzene (DVB), which were washed with 5 wt.% sodium hydroxide solution prior to use. The preparation of molecularly imprinted polymers, as illustrated in Scheme 2, was based on our recently optimized design [20] and would be

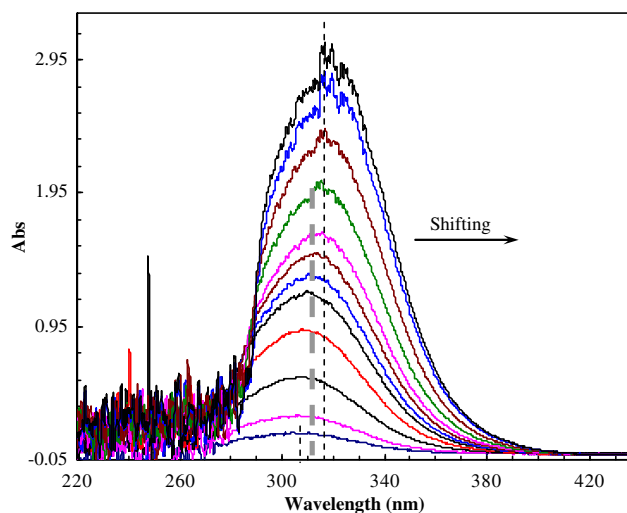


Fig. 1. The change of UV spectra as a function of the VI/NPP molar ratio.

further discussed afterward. A stoichiometric monomer–template ratio was used. NPP (0.11 g; 0.5 mmol), DVB (1.42 mL; 8.0 mmol), 1,1'-azobis(cyclohexane-1-carbonitrile) (ABCHCN) (0.60 g; 2.46 mmol), *N*-isopropylacrylamide (NIPAm) (0.91 g; 8.0 mmol) and a certain amount of VI (additionally stated) were dissolved in acetonitrile containing 50% dimethylsulfoxide (totally 10 mL) to form a homogeneous system. After being deoxygenated with sonication and nitrogen, the mixed system was irradiated by ultraviolet light (365 nm) overnight. The resulting polymers were crushed and extracted with dimethylsulfoxide containing 20% acetic acid by using a Soxhlet apparatus for 24 h. The product (i.e., MIP-S) were profusely washed with ethanol and dried at room temperature.

For comparison, three control polymers named ‘MIP’, ‘NIP’ and ‘NIP-S’ were also prepared under comparable conditions. The MIP and NIP are the conventional imprinted and non-imprinted polymers, respectively. Both of them do not have PNIPAm in their polymeric networks. The NIP-S is the non-imprinted polymer that further contains the same amount of NIPAm as it in the MIP-S.

2.2. Temperature-programmed desorption

Temperature-programmed desorption (TPD) was employed to evaluate the interaction between the prepared polymers and analyte [21,22]. Using a device comprising a gas chromatography (TCD) and a data processing system, polymers (10 mg) were placed into an online U-shaped quartz tube (4 mm ID). After 10 μ L of analyte (0.01 μ mol mL⁻¹ acetonitrile) was pre-adsorbed by these polymers, the U-shaped tube was heated under a nitrogen flow (40 mL min⁻¹; 0.23 MPa) at 10 °C min⁻¹ from room temperature to the temperature where the analyte desorbed. The desorbing signal was recorded by the data processing system.

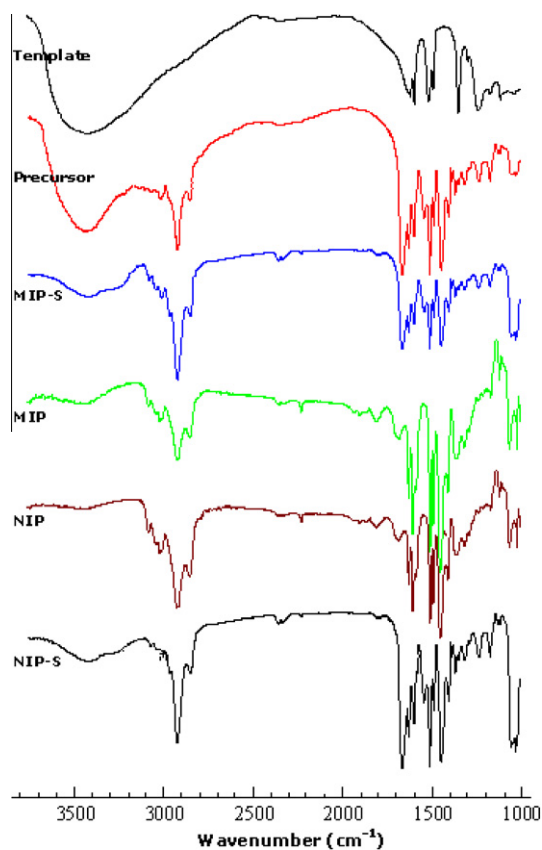


Fig. 2. FTIR spectra of the prepared polymers.

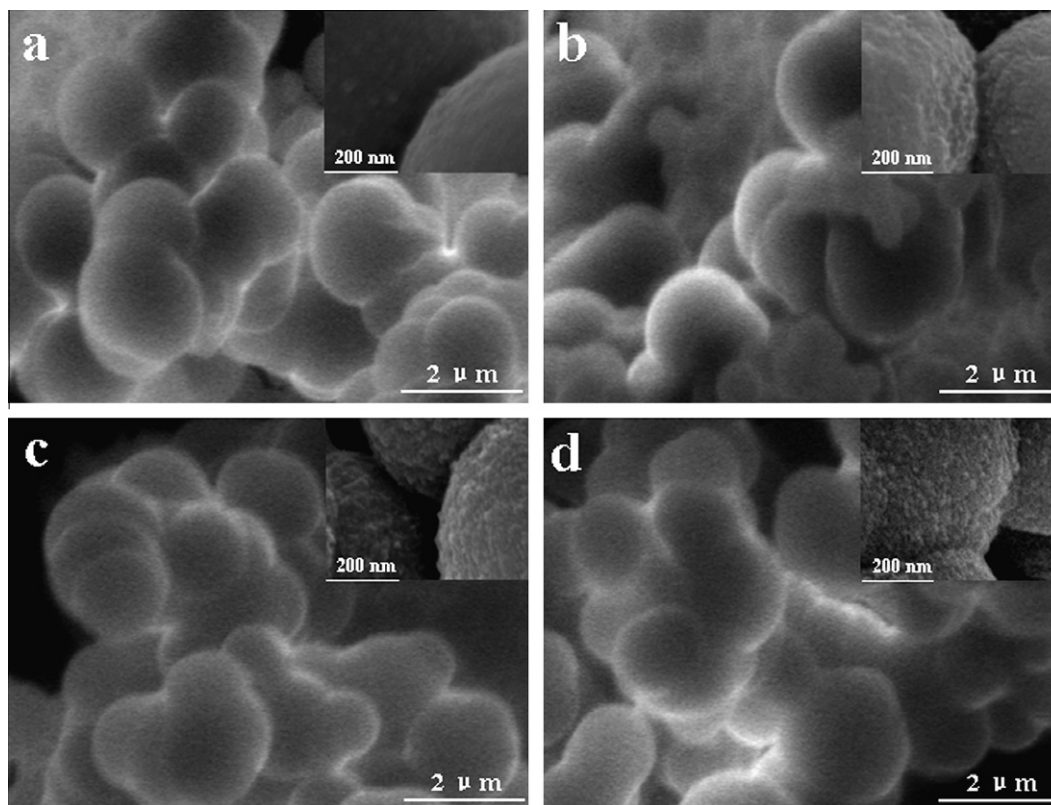


Fig. 3. SEM images of the prepared polymers. (a) NIP; (b) NIP-S; (c) MIP; (d) MIP-S.

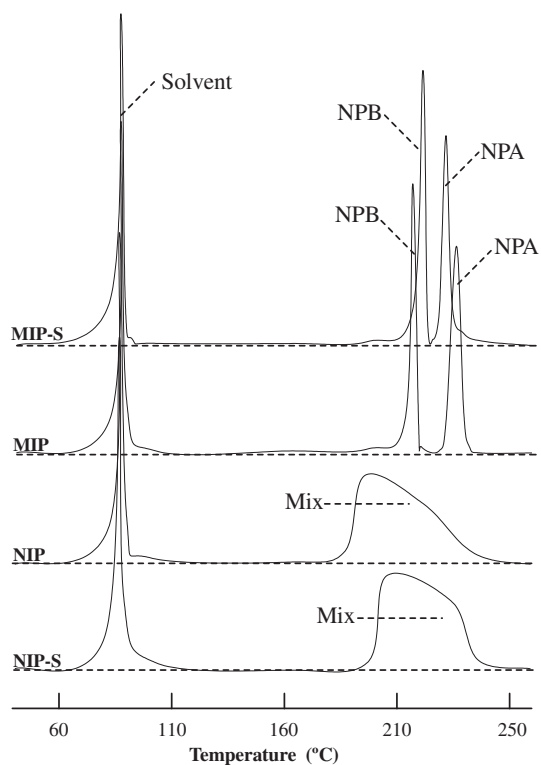


Fig. 4. TPD profiles of the prepared polymers.

2.3. Evaluation of phase transition

Dynamic light scattering (DLS) was used to evaluate the phase transition behavior in water (containing *ca.* 5% acetonitrile) [23].

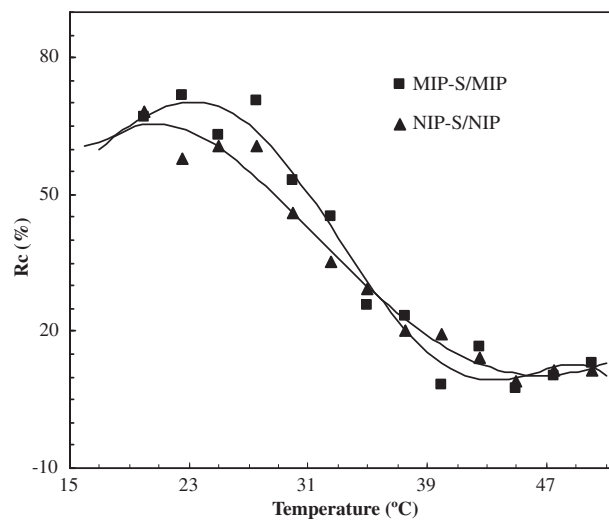


Fig. 5. DLS curves of the prepared polymers.

The DLS analysis was carried out at a scattering angle of 90° using a goniometer equipped with a self-rotation unit and a He–Ne laser (Mastersizer-X) (Malvern, UK). In order to allow equilibrium reaching, all samples were kept at specific temperatures for 10 min before acquiring the hydrodynamic radius (R_h). By a comparison between these thermosensitive and non-thermosensitive polymers, the relative change in hydrodynamic radii (R_c) reflected the contribution of the thermal phase transition:

$$R_c = \left[\left(\frac{R_h - R_d}{R_d} \right)_T - \left(\frac{R_h - R_d}{R_d} \right)_{NT} \right] \times 100\%$$

herein R_d is the particle size of dried particles. T represents the thermosensitive polymers, and NT indicates the corresponding non-thermosensitive polymers.

2.4. Catalysis test

The catalytic properties of the prepared polymers were evaluated in batch formats in PBS (pH 7.0; containing ca. 5% acetonitrile) [24]. The initial concentration of analyte (NPA or NPB) was $0.01 \mu\text{mol mL}^{-1}$ (totally 10 mL). The solid content of polymers was 2.5 mg mL^{-1} in each test. The produced *p*-nitrophenolate was spectrophotometrically monitored at 400 nm. The catalytic activity of these polymers was obtained from the average value of triple runs. By considering the effect of self-hydrolysis upon the catalysis process, the hydrolysis of analytes without any polymer was also performed under the comparable conditions, and the results were deducted from the overall activity of the prepared polymers.

2.5. Dynamic desorbing cyclic voltammetry

The potential to reduce/oxidize a binding molecule depends on the binding constant. A high binding constant requires more en-

ergy to overcome the binding, thereby leading to a larger redox potential. Thus, dynamic desorbing cyclic voltammetry (DCV) can provide valuable information on the binding interaction between the prepared polymers and their template [25,26]. Using an electrochemical workstation equipped with a three-electrode configuration (Pt-working and counter electrodes; Ag/Ag⁺-Ref.) (LK9806) (Lanlike, China), polymers (10 mg) pre-absorbed ca. $1 \mu\text{mol}$ template were placed into a cuvette encircled by a diffusion-eliminated sonication apparatus (supporting electrolyte: $0.01 \text{ mmol mL}^{-1}$ KCl; 10 mL). The transiently desorbed template was rapidly scanned by the workstation up to 20 cycles until a stable dynamic cyclic voltammogram was achieved (scanning range, ca. 800–200 mV; scanning rate, 25 mV s^{-1}).

3. Results and discussion

3.1. Template–monomer interaction and stoichiometric amount of monomer

It is well known that molecular self-assembly plays an important role in pre-determining the activity and specificity of the prepared imprinted polymer. An excess amount of monomer over the template would cause spatial and steric mismatch due to the excessive binding sites that randomly distribute throughout the polymer. On the contrary, too small an amount of monomer will result in a polymer with insufficient quantity of binding sites. Thus, only the stoichiometric amount of monomer could generate the optimal molecular recognition and catalytic ability [27]. In order to monitor this self-assembly interaction, Fig. 1 displays the UV spectrum as a function of the VI/NPP molar ratio, in which NPP (7.5 mmol L^{-1} ; $10 \mu\text{L}$ per titration) was titrated into VI (0.5 mmol L^{-1} ; 2.5 mL). The titration caused a shift in the UV spectrum, and the shift became maximal when the titrated NPP reached a critical amount (corresponding to 1.67 mol/mol VI/NPP ratio). Beyond the critical value, no further shift in the UV spectrum was observed except for increased absorbency. This result suggests that the self-assembly interaction was saturated by the stoichiometric titration, and the amount ratio of template to monomer was optimized. Thus, 0.835 mmol VI was used to prepare MIP-S and its control polymers where 0.5 mmol NPP was adopted.

3.2. FTIR spectra and SEM morphology

In order to ascertain the imprinting behavior, the FTIR spectra of MIP-S, NPP and the unwashed MIP-S system (*i.e.* the MIP-S

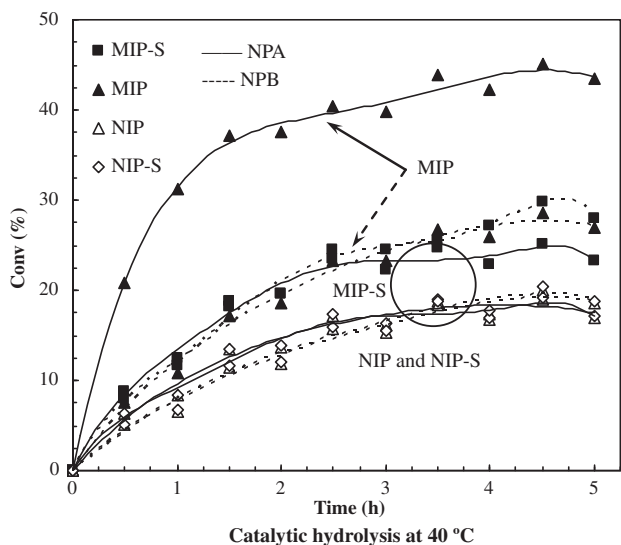
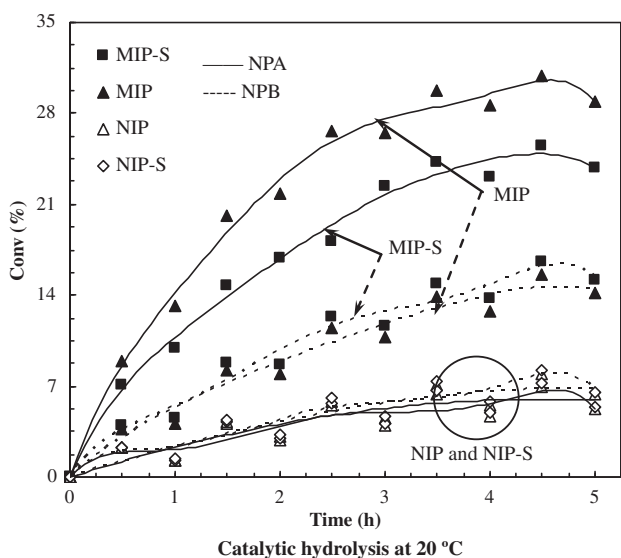


Fig. 6. Catalytic activity of the prepared polymers at 20 and 40 °C.

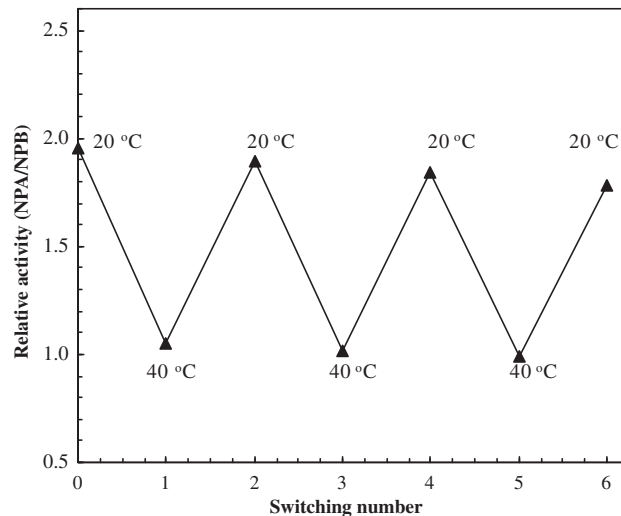


Fig. 7. Catalytic reproducibility and stability of MIP-S.

precursor) were performed (Fig. 2). Three characteristic peaks ($3200\text{--}3700$, $2800\text{--}3200$ and $1650\text{--}1750\text{ cm}^{-1}$) and one broad fingerprint band ($1000\text{--}1600\text{ cm}^{-1}$) appeared in the spectra of MIP-S and its precursor. These characteristic peaks can be assigned to the stretching vibration of O–H, C–H and C=O [28]. The fingerprint band may arise from C–N and C–C bonds and their rotation. For comparison, we also included the FTIR spectra of control polymers in Fig. 2. The MIP-S precursor, MIP-S and NIP-S all demonstrated an absorption peak at $1650\text{--}1750\text{ cm}^{-1}$, but MIP and NIP failed. This result suggests that these thermosensitive polymers did have PNIPAm in their polymeric networks [29,30]. It is noteworthy that the MIP-S precursor had the characteristic peaks of both NIP-S and NPP, implying the complicated composition of the MIP precursor. After washing, the spectrum of the MIP-S precursor (*i.e.* MIP-S) became comparable to NIP-S. This result strongly suggests that the molecular imprinting of NPP did occur during the preparation, as expected.

The SEM images of these prepared polymers are shown in Fig. 3. These polymers are spherical in morphology with similar diameters of $\sim 1.5\text{--}2\text{ }\mu\text{m}$. When compared with MIP and NIP, MIP-S and NIP-S appeared to be slightly uneven on surface. This observation probably results from the PNIPAm contained, which normally has some effects on the texture of the prepared polymers. Thus, the successful preparation of these polymers facilitates further studies.

3.3. Specific interaction between polymers and analyte

Fig. 4 presents the TPD profiles, with a purpose to further verify the interaction between the prepared polymers and analyte. Both MIP-S and MIP demonstrated significant separation abilities for NPA and NPB, but NIP and NIP-S failed. This result suggests that the interaction between the two imprinted polymers (*i.e.* MIP-S and MIP) and NPA is highly specific and capable of separation of NPA and NPB. In conjunction with the FTIR characterization, this result reflects again a consequence of the NPA-specific imprint. Since both MIP-S and MIP contained the template's 'imprint' in their polymeric networks, such molecular recognition abilities are to be expected.

3.4. Thermosensitive hydrophilicity/hydrophobicity

The DLS curves of the prepared polymers are presented in Fig. 5. In comparison with their corresponding non-thermosensitive polymers (*i.e.* MIP and NIP), MIP-S and NIP-S demonstrated more dependence on temperature, as expected. The R_c of MIP-S and NIP-S decreased with increased temperatures, indicating decreased hydrophilicity with increased temperatures. The significantly decreased hydrophilicity from MIP-S and NIP-S exhibited at *ca.* $27\text{--}37\text{ }^\circ\text{C}$. Below the temperature region, both MIP-S and NIP-S

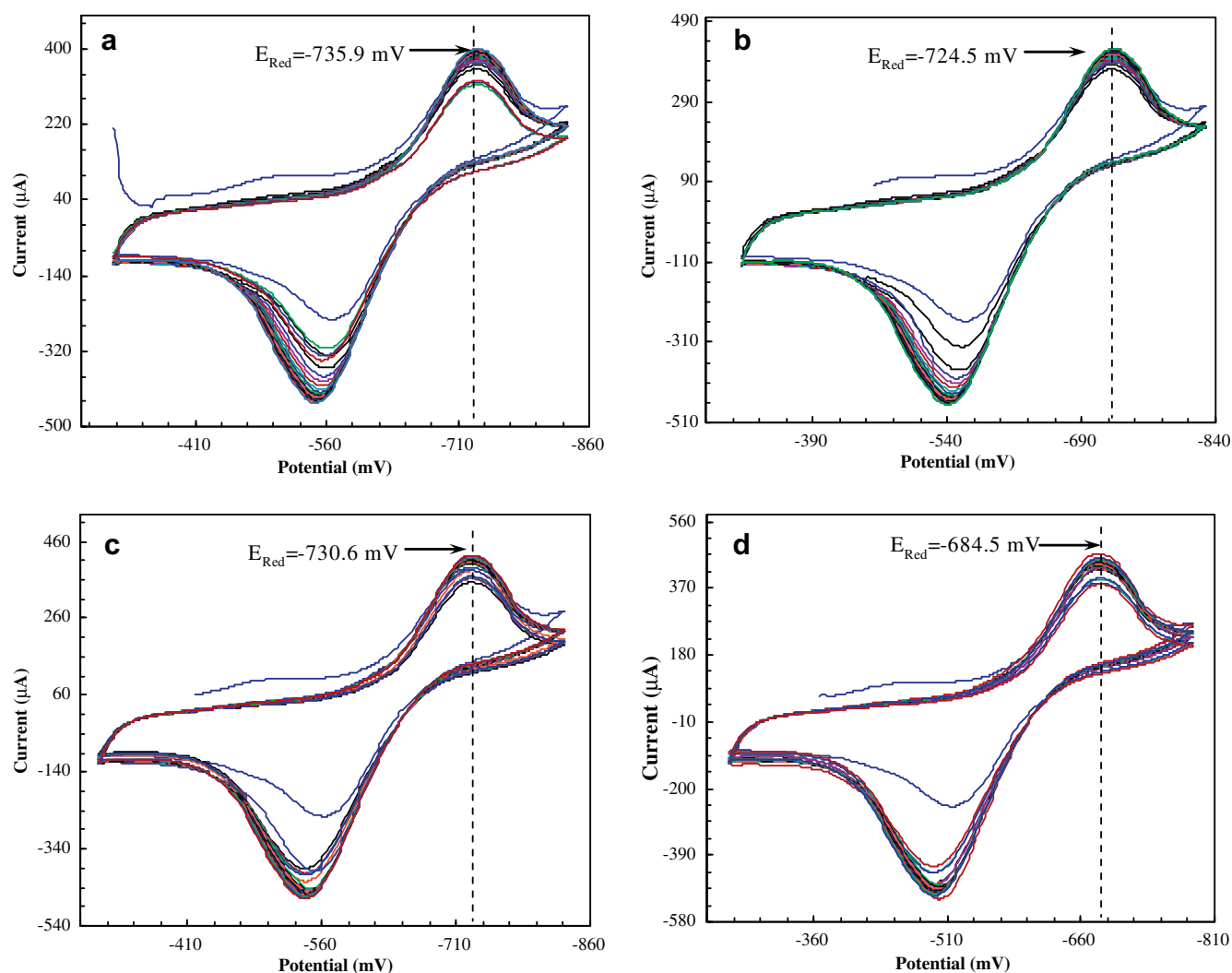


Fig. 8. DCV profiles of the template NPP with the prepared polymers. (a) MIP at $20\text{ }^\circ\text{C}$; (b) MIP at $40\text{ }^\circ\text{C}$; (c) MIP-S at $20\text{ }^\circ\text{C}$; (d) MIP-S at $40\text{ }^\circ\text{C}$; (e) NIP-S at $20\text{ }^\circ\text{C}$; (f) NIP-S at $40\text{ }^\circ\text{C}$; (g) NIP at $20\text{ }^\circ\text{C}$; (h) NIP-S at $40\text{ }^\circ\text{C}$.

exhibited relatively high hydrophilicity; however, at higher temperatures, their hydrophilicity dramatically decreased. This result, as previously explained, may be attributed to the unique thermal phase transition of PNIPAm. The higher hydrophilicity at low temperatures may be due to the hydrophilic PNIPAm networks, which allowed water to gain access to the polymer interior. The decreased hydrophilicity at higher temperatures can be attributed to the hydrophobic PNIPAm networks, which inhibited the access of water to the polymer networks.

3.5. Modulated catalysis

Fig. 6 displays the catalytic activity of the prepared polymers. In order to track the adjustable catalytic properties, herein two representative temperatures, *i.e.* 20 and 40 °C (either lower or higher than the thermosensitive region of MIP-S and NIP-S) were selected for a contrastive study. It was observed that MIP-S at 20 °C was comparable to MIP and capable of vigorous catalysis for the hydrolysis of NPA. However, MIP-S at 40 °C was more like NIP-S and NIP, which did not demonstrate significant specific catalysis. MIP-S apparently demonstrated the thermo-switchable catalytic properties. Clearly, this result can be attributed to the unique thermal sensitivity of the MIP-S networks. The hydrophilic MIP-S networks at the low temperature allowed reactants to gain access to the

polymer networks, which thereby enabled the vigorous catalysis. Above the transition temperature, the dramatically decreased hydrophilicity inhibited the access of water to the polymer networks, thus inhibiting the catalytic activity.

Fig. 7 illustrates the catalytic reproducibility and stability of MIP-S. The reactivity of MIP-S did not demonstrate significant decrease after a series of 'on/off'-switched catalysis. This result suggests that MIP-S is relatively stable and capable of reproducing the switchable catalysis. Clearly, the catalytic reproducibility and stability of MIP-S can be attributed to the highly cross-linked imprinted networks. Molecularly imprinted polymers, as previously explained, are highly cross-linked polymers, which offer significant advantages of stabilizing the imprinted conformation. Hence, the catalytic reproducibility of MIP-S could be expected.

3.6. Switchable binding behavior

As previously pointed out, the DCV experiments may provide valuable information on the binding behavior of molecularly imprinted polymers with their template. By considering the thermosensitive mechanism of MIP-S, we further selected 20 and 40 °C for a contrastive study. As shown in Fig. 8, the template molecule (*i.e.* NPP) bound to MIP-S at 20 °C exhibited a reduction peak at -730.6 mV (Fig. 8c). In contrast, this reduction peak at 40 °C

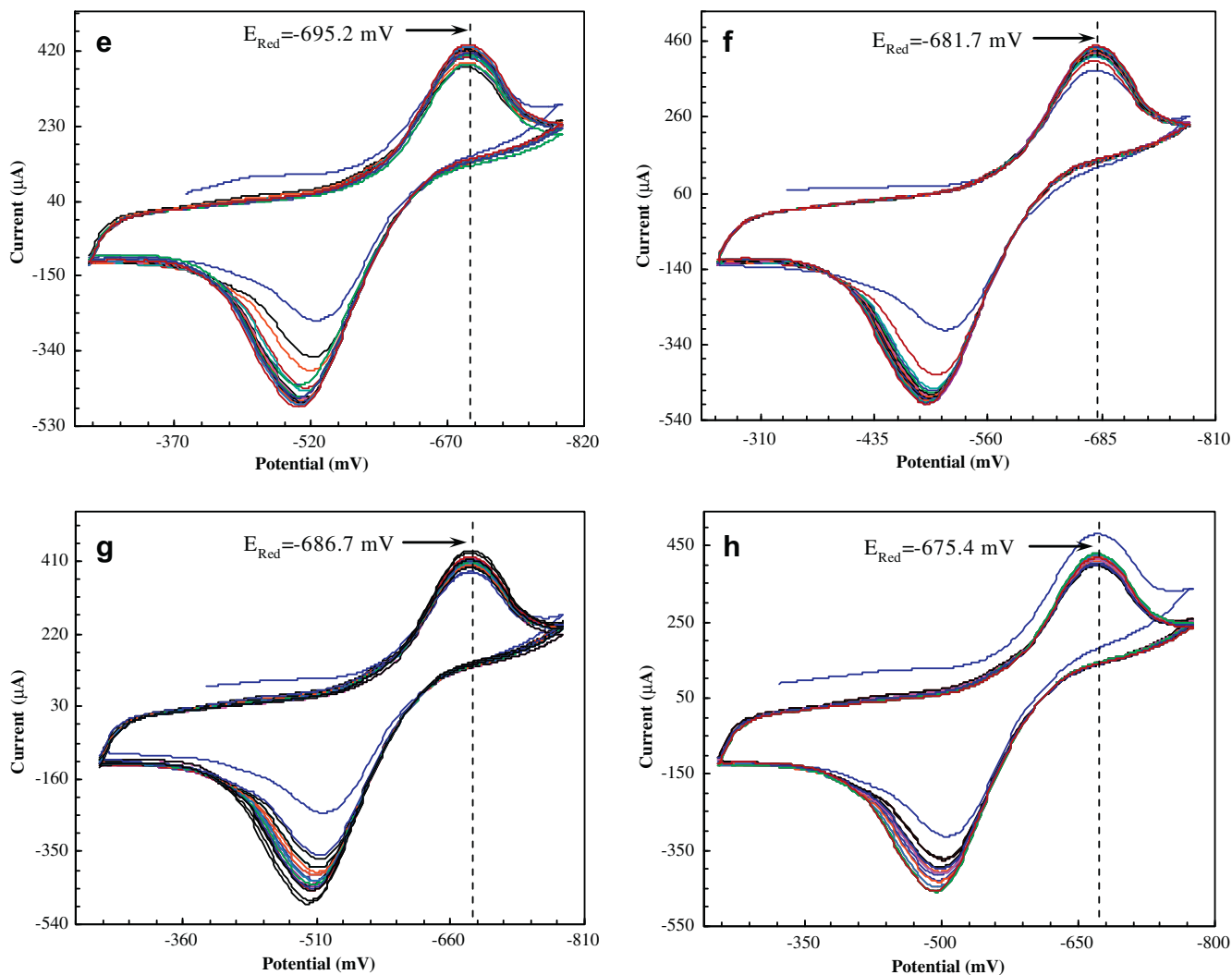


Fig. 8 (continued)

shifted to a smaller Fig. (i.e., -684.5 mV) (Fig. 8d). MIP-S demonstrated a weaker interaction with its template molecule at 40 °C than at 20 °C.

In order to clarify this interaction, Fig. 8a, b, e, f, g and h also included the reduction potentials of the template molecule from these control polymers. The reduction potential of the template bound to MIP-S at 20 °C was nearly comparable to that from MIP (-730.6 vs. -735.9 mV). The reduction potential of the template bound to MIP-S at 40 °C became as low as that from NIP-S (-684.5 vs. -681.7 mV). The results strongly suggest that MIP-S did provide a thermo-switchable interaction with its template molecule. Again, this result can be attributed to the unique thermal sensitivity of the MIP-S networks. The thermosensitive mechanism by MIP-S regulated the access of analyte to the imprinted networks, which thereby enabled the switched binding.

4. Conclusions

'On/off'-switchable catalysis by a smart enzyme-like imprinted polymer is reported in this study. This unique polymer was composed of poly(*N*-isopropylacrylamide)-containing molecularly imprinted networks that exhibited temperature-dependent hydrophilicity/hydrophobicity. By creating such a hydrophilic/hydrophobic transition within the imprinted networks, the prepared MIP-S was capable of 'on/off'-regulated access to the reactants, leading to switchable catalysis. At relatively low temperatures, this polymer demonstrated vigorous catalysis. However, at relatively high temperatures, this polymer exhibited poor reactivity. The results demonstrate that switchable catalysis by the smart and catalytic imprinted polymer can be realized by using this novel design. By taking advantages of the excellent stability, cost-effectiveness, ease of preparation and reusability of molecular imprinting technology, the resulting system could offer tantalizing applications toward substantial and self-control catalysis.

Acknowledgments

The authors thank the Research Directorate-General of European Commission for supporting this work under the framework of Marie Curie Actions (PIIF-GA-2009-236799, 254955 and

254957). Similar thanks are expressed to the National Science Foundation of China (No. 21073068).

References

- [1] R.N. Liang, D.A. Song, R.M. Zhang, W. Qin, *Angew. Chem. Int. Ed.* 49 (2010) 2556–2559.
- [2] F. Yanez, I. Chianella, S.A. Piletsky, A. Concheiro, C. Alvarez-Lorenzo, *Anal. Chim. Acta* 659 (2010) 178–185.
- [3] Y.J. Zhao, X.W. Zhao, J. Hu, J. Li, W.Y. Xu, Z.Z. Gu, *Angew. Chem. Int. Ed.* 48 (2009) 7350–7352.
- [4] K. Wybranska, W. Niemiec, K. Szczubialka, M. Nowakowska, Y. Morishima, *Chem. Mater.* 22 (2010) 5392–5399.
- [5] B.T.S. Bui, F. Merlier, K. Haupt, *Anal. Chem.* 82 (2010) 4420–4427.
- [6] P. Pasetto, K. Flavin, M. Resmini, *Biosens. Bioelectr.* 25 (2009) 572–578.
- [7] J.Q. Liu, G. Wulff, *J. Am. Chem. Soc.* 126 (2004) 7452–7453.
- [8] Y. Lu, Y. Mei, M. Drechsler, M. Ballauff, *Angew. Chem. Int. Ed.* 23 (2006) 813–816.
- [9] S. Schilp, N. Ballav, M. Zharnikov, *Angew. Chem. Int. Ed.* 47 (2008) 6786–6789.
- [10] S.W. Choi, Y. Zhang, Y. Xia, *Angew. Chem. Int. Ed.* 49 (2010) 7904–7908.
- [11] D.E. Bergbreiter, P.L. Osburn, A. Wilson, E.M. Sink, *J. Am. Chem. Soc.* 122 (2000) 9058–9064.
- [12] D.E. Bergbreiter, Y.S. Liu, P.L. Osburn, *J. Am. Chem. Soc.* 120 (1998) 1250–1251.
- [13] T. Sun, G. Wang, L. Feng, B. Liu, Y. Ma, L. Jiang, D. Zhu, *Angew. Chem. Int. Ed.* 43 (2004) 357–360.
- [14] H. Ko, Z. Zhang, Y.L. Chueh, E. Saiz, A. Javey, *Angew. Chem. Int. Ed.* 49 (2010) 616–619.
- [15] S. Li, S. Pilla, S. Gong, *J. Polym. Sci. Part A: Polym. Chem.* 47 (2009) 2352–2360.
- [16] Z. Chen, L. Xu, Y. Liang, M. Zhao, *Adv. Mater.* 22 (2010) 1488–1492.
- [17] Z. Chen, Z. Hua, L. Xu, Y. Huang, M. Zhao, Y. Li, *J. Mol. Recognit.* 21 (2008) 71–77.
- [18] P. Pasetto, S.C. Maddock, M. Resmini, *Anal. Chim. Acta* 542 (2005) 66–75.
- [19] K. Lettau, A. Warsinke, A. Laschewsky, K. Mosbach, E. Yilmaz, F.W. Scheller, *Chem. Mater.* 16 (2004) 2745–2749.
- [20] D. Zhang, S. Li, W. Li, Y. Chen, *Catal. Lett.* 115 (2007) 169–175.
- [21] S. Li, S. Gong, *Adv. Funct. Mater.* 19 (2009) 2601–2606.
- [22] S. Li, S. Gong, *J. Phys. Chem. B* 113 (2009) 16501–16507.
- [23] S.V. Ghugare, E. Chiessi, M.T.F. Telling, A. Deriu, Y. Gerelli, J. Wuttke, G. Paradossi, *J. Phys. Chem. B* 114 (2010) 10285–10293.
- [24] S. Li, K. Tong, D. Zhang, X. Huang, *J. Inorg. Organomet. Polym.* 18 (2008) 264–271.
- [25] S. Li, A. Tiwari, Y. Ge, D. Fei, *Adv. Mater. Lett.* 1 (2010) 4–10.
- [26] S. Li, X. Huang, M. Zheng, W. Li, *Anal. Bioanal. Chem.* 392 (2008) 177–185.
- [27] B.C.G. Karlsson, J. O'Mahony, J.G. Karlsson, H. Bengtsson, L.A. Eriksson, I.A. Nicholls, *J. Am. Chem. Soc.* 131 (2009) 13297–13304.
- [28] W. Wang, X. Tian, Y. Feng, B. Cao, W. Yang, L. Zhang, *Ind. Eng. Chem. Res.* 49 (2010) 1684–1690.
- [29] S. Lv, L. Liu, W. Yang, *Langmuir* 26 (2010) 2076–2082.
- [30] M. Recillas, L.L. Silva, C. Peniche, F.M. Goycoolea, M. Rinaudo, W.M. Arguëlles-Monal, *Biomacromolecules* 10 (2009) 1633–1641.